JOURNAL OF CATALYSIS 48, 8–20 (1977)

On the Hydrogenation of Olefins with Tetrachloro Palladate Catalysts

A Molecular Orbital Study of the Reaction Pathway

D. R. ARMSTRONG,[1] AND O. NOVARO

Instituto de Fisica, Universidad Nacional Autonoma de Mexico, Apdo. 20-364, Mexico, D. F.; and Instituto Mexicano del Petroleo, Av. Cien Metros 152, Mexico 14, D. F.

AND

M. E. RUIZ-VIZCAYA AND R. LINARTE

Instituto Mexicano del Petroleo, Av. Cien Metros 152, Mexico 14, D. F.

Received March 1, 1976; revised February 14, 1977

The catalytic hydrogenation of styrene in the presence of tetrachloropalladate catalysts has been studied by an all-valence-electron self-consistent-field method. A molecular orbital description of the following reaction sequence is presented: the heterolytic breaking of a hydrogen molecule by the catalyst $[PdCl_4]^{2-}$ complex with a subsequent substitution of a chlorine by a hydrogen, the coordination of the olefin to the planar $[PdCl_3H]^{2-}$ complex, the movement of the coordinated olefin through a collapse mechanism towards the hydride, and the final hydrogenation through an acid attack (HCl) on the Pd–alkyl bond liberating the alkane and regenerating the catalytic species $[PdCl_4]^{2-}$. Each reaction step is justified through the analysis of the energies and charge distributions. A satisfactory theoretical explanation of the proposed reaction mechanism is presented.

I. INTRODUCTION

Palladium(II) compounds are chemically and commercially important due to the versatility of their catalytic properties. Reactions which occur in the presence of these compounds include the hydroesterification, hydrogenation, isomerization and oxidation of olefins (*1*). Currently, our understanding of the electronic interactions and the orbital involvement which exist in these processes is very sparse and therefore to amplify our knowledge of this significant area of chemistry we present the results of a molecular orbital study of one of these processes, namely, the hydrogenation of styrene catalyzed by the anion $[PdCl_4]^{2-}$. The mechanism of the process was established by an experimental study which led to a kinetic model of reaction rates (*2*). The model is schematically represented in Fig. 1 as a series of reactions. Calculation of the electronic structure of the species at points in the paths of the reactions would therefore produce an insight into the reaction mechanism and provide evidence for the validity of the model.

The experimental investigation was actually carried out as a heterogeneous process in which the catalyst was chemically supported $[PdCl_4]^{2-}$/A-27(OH^-), (*3–5*). It is not yet possible to attempt a thorough

[1] Permanent address: Department of Pure and Applied Chemistry, University of Strathclyde, Glasgow, Scotland, United Kingdom.

ISSN 0021-9517

theoretical study of a solid catalyst species. Therefore, in this study it was necessary to employ a "soluble" $[PdCl_4]^{2-}$ complex. We feel, however, that for this type of complex, no profound difference exists between the heterogeneous and homogeneous processes (*3–5*).

II. METHOD

The calculations were performed within a modified CNDO version (*6*) of the all-valence electron SCF–MO approach. The method has been employed in previous successful investigations of catalytic systems using transition metal complexes (*7–10*). The atomic input parameters are displayed in Table 1, while the molecular coordinates of the reactant and product were obtained from the literature (*11*).

Preliminary calculations on $[PdCl_4]^{2-}$ revealed that the charge on the chlorine atoms, -0.56, is in fairly good agreement with the experimental value, -0.67, estimated from NQR measurements (*12*). The excited states of $[PdCl_4]^{2-}$ were computed and are presented in Table 2. The agreement with experiment (*13–15*), especially of the allowed bands, can reasonably be taken to indicate the general acceptability of the input parameters.

III. RESULTS AND DISCUSSION

Before analyzing the proposed reaction coordinates, it is desirable to discuss the electronic structure of $[PdCl_4]^{2-}$. In our calculations, we propose to use an isolated complex with a net negative charge. Now, it is well known that the effects of the solvent and the chemical support in the homogeneous and heterogeneous case, respectively, balance this high negative charge. Therefore, our first priority was to establish that these effects would merely change the absolute values of the total energy and molecular orbital energies and neither change the order of orbitals nor drastically alter the orbital populations. Trial calculations were accordingly performed on both an isolated $[PdCl_4]^{2-}$ species and on $[PdCl_4]^{2-}$ in an elementary cell of K_2PdCl_4 solid. The resulting Pd *p*- and *d*-orbital populations and Cl *p*-orbital population for both moieties are presented in Table 3. It can be seen that no major

TABLE 1

Atomic Orbital Input Parameters

	Valence state ionization potentials (eV)			Orbital exponents			One-center two-electron integral (eV)		
	s	*p*	*d*	*s*	*p*	*d*	*s*	*p*	*d*
Pd	7.28	3.69	8.33	1.34	0.72	2.83	7.3		
Cl	25.29	13.99		2.183	1.733		15.3		
C	19.44	10.67		1.55	1.325		15.6		
H	13.60			1.0			17.0		

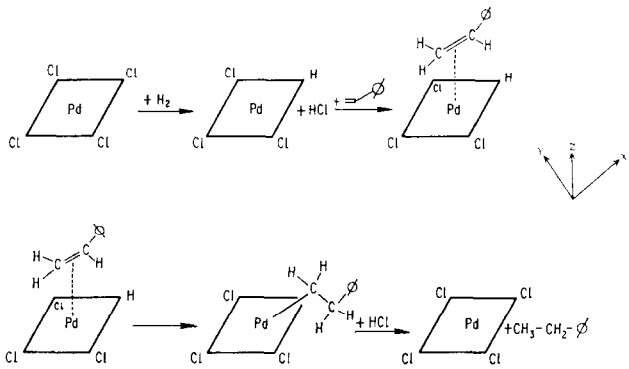

FIG. 1. Reaction mechanism for the catalytic hydrogenation of styrene.

TABLE 2

Calculated and Experimental Electronic Transitions for $[PdCl_4]^{2-}$

Experimental transition energies (eV)	Extinction coefficient	Calcd transition energies (eV)	Oscillator strength
2.48	67	2.09	0.0
2.78	125	2.20	0.0
3.74	67	2.38	0.0
4.46	12,000	4.96	0.14
5.60	28,200	5.51	0.41

changes in the electronic populations are produced by the inclusion of the neighboring positive charges. Furthermore, inspection of the molecular orbital ordering of the neutral and anionic species reveals that they are identical (Fig. 2). Hence we are confident that our analysis of the reaction coordinate will be realistic.

The hydrogenation process outlined in Fig. 1 can be conveniently divided into four main sequences, namely, the heterolytic scission of a hydrogen molecule with the subsequent liberation of HCl and formation of a $[PdCl_3H]^{2-}$ complex, the coordination of the olefin to this complex, followed by its later movement towards the hydrogen, with the creation of an alkyl group, and finally, the attack by

TABLE 3

The Valence Electron Density Distribution of $[PdCl_4]^{2-}$ [a]

	$PdCl_4^{2-}$	K_2PdCl_4
Pd *s*	0.53	0.56
p	0.56	0.46
d	8.67	8.53
Cl *s*	1.85	1.92
p	5.71	5.69

[a] As an isolated molecule and present in a K_2PdCl_4 simple cell.

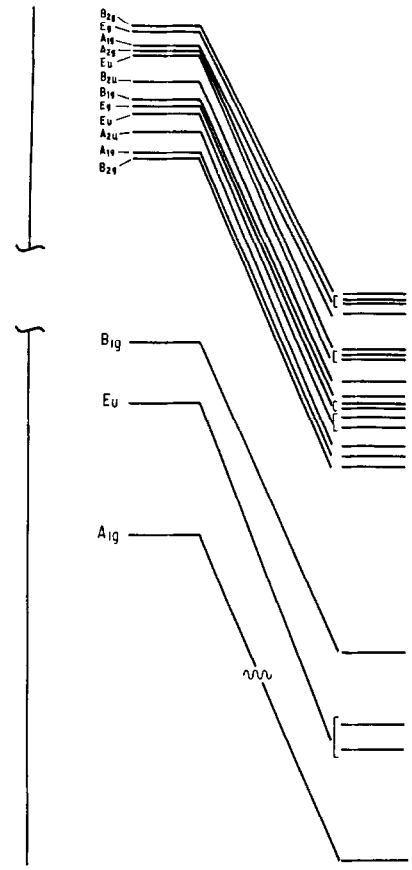

FIG. 2. Molecular orbital energy ordering for the $[PdCl_4]^{2-}$ complex (square planar symmetry) and for the K_2PdCl_4 crystal cell.

HCl with the ensuing release of the alkane and the production of $[PdCl_4]^{2-}$. In the experimental studies of this reaction there is no information to distinguish between two plausible mechanisms for stage III. In the aforegoing outline we stated that the coordinated olefin moves towards the hydrogen. It is also possible that the hydrogen advances towards the olefin. Preliminary calculations, however, reveal that a high activation barrier is created during the movement of the hydrogen while the progress of the olefin produces a gain in stability of the system. (We say that this stage involves a collapse mechanism because the complex regains a planar structure).

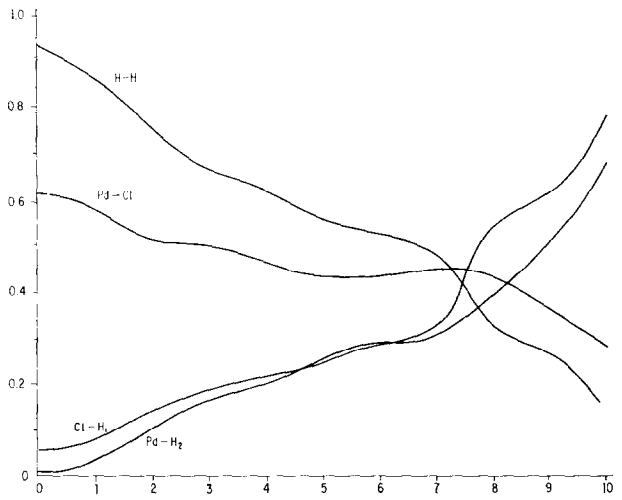

FIG. 3. Changes in the bond orders during the heterolytic breaking of H_2 by the catalytic complex. The 11 steps of Table 4 are successively given by Nos. 0 to 10 in the abcissa.

a. Reaction between H_2 and $[PdCl_4]^{2-}$

The hydrogen molecule approaches the palladium coordination sphere above a palladium chlorine bond. The H–H bond is then allowed to increase, with an accompanying decrease in the H–Cl distance. Table 4 reports the relevant bond distances and also the net changes on the hydrogen atoms. The changes in the related bond indices (*16*, *17*) are displayed in Fig. 3. The bond index B_{AB} between two atoms A and B is defined as

$$B_{AB} = \sum_{\mu \text{ on A}} \sum_{\sigma \text{ on B}} P_{\mu\sigma}^2,$$

where $P_{\mu\sigma}$ is a density matrix element. This bonding parameter is a useful quantity with which to categorize the bonding between atoms A and B, since it signifies the multiplicity of the bond, e.g., bond indices of 1, 2, 3 are calculated for the C–C bonds in C_2H_6, C_2H_4 and C_2H_2, respectively (*16*, *17*).

The charge polarization and the weakening of the H–H bond appears even before relaxation of the H–H distance is initiated. As the reaction proceeds, H_2, the atom closer to the Pd, becomes increasingly negatively charged while H_1, the atom directed towards a chlorine atom, gradually acquires a positive charge. This is accompanied by a progressive increase in the Pd–H_2 and Cl–H_1 bond strength, with a concomitant weakening of the Pd–Cl and H_1–H_2 bonds. Figure 3 represents the bond description of a heterolytic breaking of molecular hydrogen, whereby a positively charged hydrogen (+0.23) combines with a negatively charged chloride ion while the

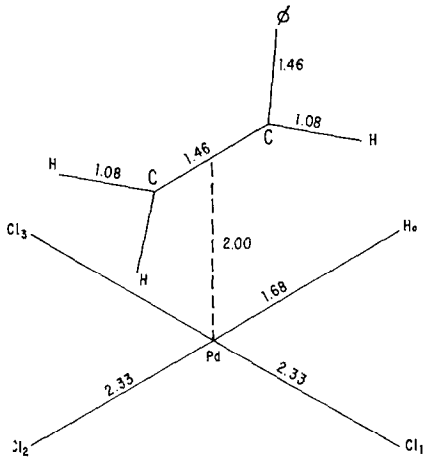

FIG. 4. Interatomic distances in the [olefin–$PdCl_3H]^{2-}$ complex.

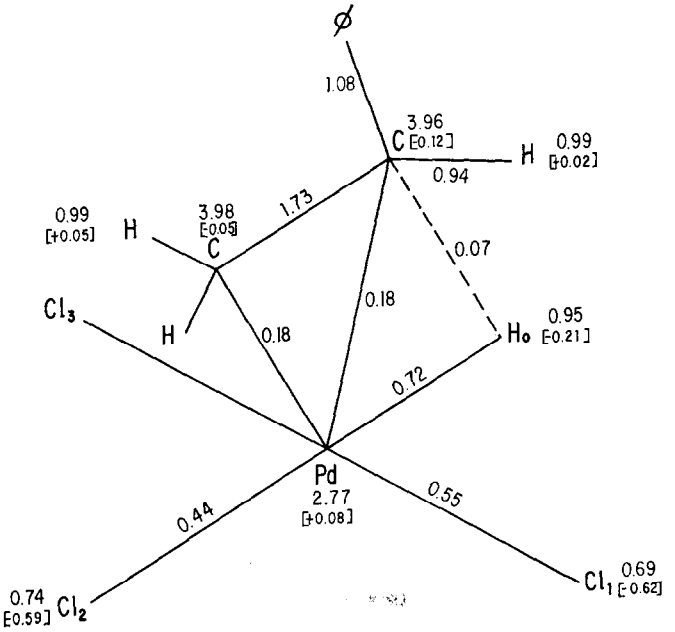

FIG. 5. Charge distribution of [olefin–$PdCl_3H$]$^{2-}$ bond orders, atomic valencies and net charges (in brackets) are given.

negatively charged hydrogen replaces a chlorine in the planar complex with the formation of [$PdCl_3H$]$^{2-}$. Perhaps the most interesting aspect of this diagram is the materialization of the transition state as a multiple crossing point between the 7th and 8th step's of the reaction sequence. At this situation we find the H–H distance to be between 1.10 and 1.15 Å and the H–Cl bond length is between 1.60 and 1.62 Å, an increase for both bond measurements of 0.3–0.4 Å over the diatomic internuclear distance.

b. Styrene Coordination

In this section we analyze the coordination of the olefin to the [$PdCl_3H$]$^{2-}$ species. The styrene enters the bonding sphere of the palladium so that the olefinic bond lies along the x-axis and the center of the bond coincides with the z-axis. (Fig. 4). The valencies (*16, 17*) and net charges of each atom together with the bond indices of this pentacoordinated complex are displayed in Fig. 5. It can be seen that there is a small net transfer of electronic charge to the

TABLE 4

Charge Polarization of the H_1–H_2 bond

	Reaction step										
	1	2	3	4	5	6	7	8	9	10	11
H_1–Cl distance (Å)	2.44	2.33	1.75	1.69	1.65	1.62	1.62	1.60	1.51	1.43	1.29
H_1–H_2 distance (Å)	0.74	0.74	0.74	0.79	0.95	0.95	1.1	1.15	1.2	1.2	1.29
H_1[a] charge	+0.035	+0.026	+0.089	+0.133	+0.139	+0.143	+0.143	+0.160	+0.177	+0.202	+0.229
H_2[b] charge	+0.025	+0.020	−0.044	−0.056	−0.132	−0.133	−0.168	−0.197	−0.235	−0.257	−0.277

[a] H_1 is the hydrogen atom closer to the chloride.
[b] H_2 is the hydrogen atom closer to the palladium.

TABLE 5

Dominant Contributions of the Five Highest Occupied Molecular Orbitals of the Penta-Coordinated Complex $[Pd\ Cl_3H\ Styrene]^{2-}$ (see text)[a]

Molecular orbital	Atomic orbital coefficients									
	Palladium					α-Carbon (C_1)		β-Carbon (C_2)		Hydride
	$d_{x^2-y^2}$	d_{xz}	d_{z^2}	d_{yz}	d_{xy}	p_x	p_z	p_x	p_z	s
ψ_1	−0.2	−0.10	−0.67	—	—	—	−0.29	—	−0.35	−0.14
ψ_2	—	—	—	+0.92	+0.15	—	—	—	—	—
ψ_3	−0.1	+0.58	−0.14	—	—	+0.07	−0.06	−0.06	+0.04	−0.36
ψ_4	—	—	—	−0.14	+0.91	—	—	—	—	—
ψ_5	−0.2	−0.44	+0.34	—	—	−0.14	−0.19	+0.17	+0.07	−0.38

[a] These orbitals are called, in order of decreasing energy ψ_1, ψ_2, ψ_3, ψ_4, and ψ_5.

olefin upon coordination. This is accompanied by the appearance of small palladium–olefinic carbon bond indices and a decrease in the olefinic bond index from the noncoordinated value of 2 to 1.7. The valencies of both the β-carbon atom (C_2) of the olefinic bond and the hydrogen atom of the $[PdCl_3H]^{2-}$ species are lower than normal (*16*, *17*) indicating that these atoms are relatively unsaturated and hence are positions of reactivity. The bond indices of the palladium–ligand bonds are appreciably lower than unity as is usual in these highly ionic complexes. It is of interest to note that the Pd–Cl_2 bond *trans* to hydrogen is weaker than the other Pd–Cl bonds. As there is also a small bond index between C_1 (the α-carbon atom) and Cl_2 (not shown in Fig. 5) the possibility of an olefin—chlorine interaction or displacement is quite possible and must therefore be considered. A series of computations reveals that movement of the olefin towards the chlorine creates a high energy barrier. The presence of this high activation barrier produces important implications. First, the heterolytic breaking of H_2 does not have to precede the coordination of the olefin. This means that if we initially consider an olefin coordinated to $[PdCl_4]^{2-}$ the later entrance of H_2 and the heterolytic scission of the hydrogen bond will not be hindered by the configuration as the olefin cannot move towards the chlorines because of the energy barrier. This energy barrier may also account for the very slow formation of Zeise-type anions with $[PtCl_4]^{2-}$ and $[PdCl_4]^{2-}$ whose formation is actually favored only when some ligands other than chloride ions are present (*18*). Finally we can conclude that the only displacement left for the olefin is towards the hydrogen.

TABLE 6

Variation of the Bond Indices between the Palladium d_{xz} Orbital and the Hydrogen s Orbital, the Carbon 1 p orbitals, and the Carbon 2 p Orbitals over the Reaction Steps of the Collapse Reaction

Bond	Reaction step						
	0	1	2	3	4	5	6
H s–Pd d_{xz}	0.0044	0.0273	0.0262	0.0019	0.0079	0.0017	0.0000
C_2 p–Pd d_{xz}	0.0827	0.0869	0.0085	0.0058	0.0016	0.0010	0.0004
C_1 p–Pd d_{xz}	0.0760	0.0670	0.0046	0.0135	0.1075	0.0285	0.0017

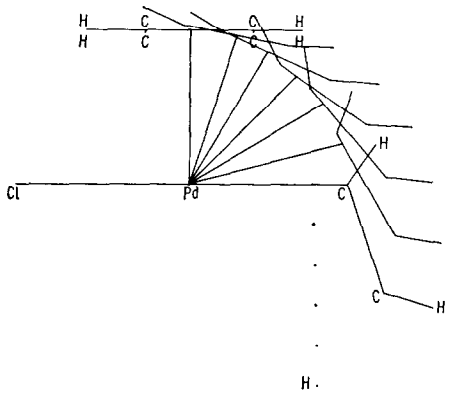

FIG. 6. Collapse reaction. Schematic representation of the movement, in seven steps, of the olefin towards the coordinated hydrogen.

The major atomic orbital contributions of the five highest occupied molecular orbitals are reported in Table 5. For simplicity the orbital coefficients of the chlorine atoms are not included. Although they are not negligible they remain almost constant over the reaction coordinate of the hydrogenation process and so they do not represent any relevant influence in the chemical mechanisms which are of interest. The lowest lying of these five orbitals (we shall call it ψ_5) is by far the most important with regard to the olefin–palladium bonding situation. ψ_5 provides Pd–olefin bonding through the interaction of the Pd d_{z^2} and d_{xz} orbitals with the p_x and p_z orbitals of the olefinic α- and β-carbon atoms. Of particular interest are the opposite signs of the p_z orbitals of the olefinic carbon atoms. This allows positive overlapping of these orbitals with the corresponding lobes of the d_{xz} orbital but negative overlap between the carbon atoms. They are therefore contributing to the π^*-orbital of the ethylene. Here we observe, therefore, an important back-donation effect of the type predicted by Cossee (*19*) and which explains the aforementioned decrease in the bond index between these carbons.

The next three molecular orbitals ψ_2, ψ_3, and ψ_4 are essentially nonbonding as regards the Pd–olefin interaction. These three orbitals are basically Pd d_{yz}, d_{xz} and d_{xy} in order of increasing energy although the second one, ψ_3, has a small contribution from d_{z^2} and $d_{x^2-y^2}$ and the hydrogen s orbital thus subscribing also to Pd–H bonding (as do ψ_1 and ψ_5). The form of the highest occupied molecular orbital ψ_1 is quite interesting as it is composed of the Pd d_{z^2} orbital and the p_z orbitals of the olefinic carbon atoms. The signs of these coefficients indicate that this interaction is antibonding with respect to the Pd–olefin

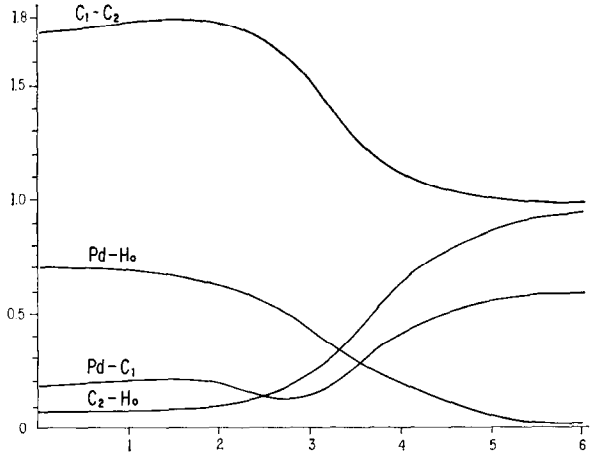

FIG. 7. Changes in the bond indices during the collapse. The seven steps of Fig. 6 correspond to the numbers 0 to 6 in the abcissa.

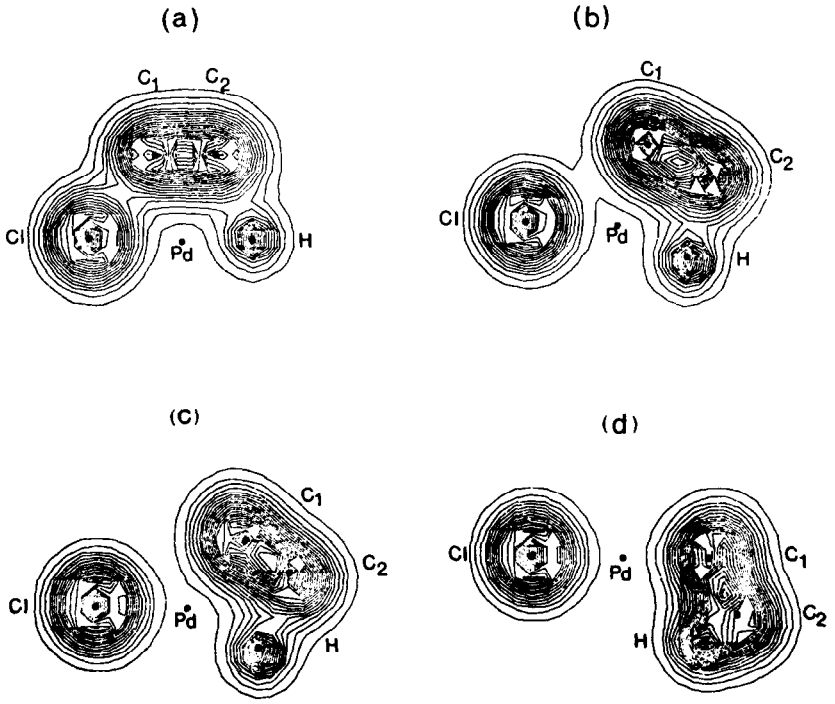

FIG. 8. Total electron density contour plots for four steps (0, 2, 4, 6) of the collapse reaction.

bond. We consider this to be an important characteristic of this complex as this molecular orbital effectively labilizes such a bond. In other words the two excess electrons of the dianion go into this orbital facilitating the olefin's possible displacement.

In previous studies (*7–9, 20*) on several other catalytic processes we have encountered a situation where the molecular orbital which directly contributes to the bonding of the most labile ligand (the one that usually performed a *cis*-migration as the catalyzed reaction proceeded) is always the highest occupied one. In this hydrogenation process the dianionic charge is crucial as it means that the two extra electrons go into an antibonding molecular orbital thus labilizing the Pd–olefin bond. The absence of these electrons would imply that the highest filled orbitals would be the nonbonding (d_{xy}, d_{xz} and d_{yz}) orbitals. The highest occupied orbital which is concerned with palladium–olefin bonding can therefore be correlated with the preferred movement of the olefin towards the hydrogen. This is in contrast to the Ziegler-Natta process where the highest occupied orbital is localized about the titanium–alkyl bond and is interconnected with the movement of the alkyl species towards the olefin (*7, 8*).

c. Collapse Mechanism

The "collapse" reaction path was divided into seven successive steps for calculational purposes and these are depicted in Fig. 6. It was found at each of these steps that the total energy of the system was lowered and so no activation energy barrier to the movement of the olefin is present. The decrease in the total energy of the system during the formation of the alkyl group is the driving force of the reaction. This answers the most crucial question of the hydrogenation process, namely, why this reac-

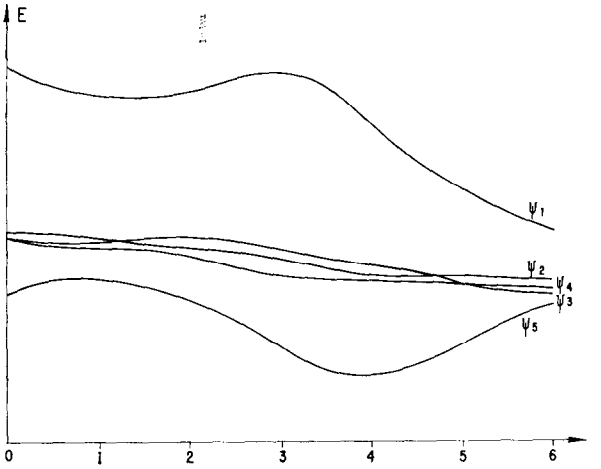

FIG. 9. Orbital energies over the collapse reaction coordinate. Only the five highest occupied molecular orbitals are represented.

tion, which in the absence of the catalyst implies a prohibitively high activation barrier, occurs so readily in the presence of $[PdCl_4]^{2-}$. We must remember that the free movement of the olefin is possible only when a hydrogen atom is present on the coordination site and, furthermore, that the inverse movement of the hydrogen towards the olefin is highly unfavored.

The changes in the relevant bond indices over the reaction path are illustrated in Fig. 7 while the total electron density contour plots at four points of the reaction coordinate are displayed in Fig. 8. The Pd–H, and C_2–H_1 bond indices smoothly decrease and increase, respectively. The C_1–C_2 bond becomes a single bond at the end of the reaction path although the C_1–C_2 bond index increases as the styrene starts its movement. This augmentation can be readily explained by reference to the back-donation effects on the palladium–olefin bond. As the styrene moves, the electron-migration towards the olefin is less important because no d orbital on the Pd atom can play the role that the d_{xz} orbital performed in the initial coordinated intermediate structure. The very conspicuous weakening of the Pd–C_1 bond index at the middle step of the collapse reaction is discussed further in the analysis of the individual molecular orbitals. We also observe that bond-breaking occurs simultaneously with the formation of new bonds and hence the absence of an energy barrier can be rationalized in terms of the latter processes providing more than sufficient energy for the former reactions to take place. The increasing interaction between H and C_2 over the reaction coordinate is well illustrated by the electron density plots of Fig. 8.

The changes in the energies of orbitals ψ_1 to ψ_5 over the reaction path of stage III are presented in Fig. 9. It can be seen that the energies of ψ_1 and ψ_5 alter quite considerably over the reaction coordinates. The energy of ψ_3 varies slightly while the energy of ψ_2 and ψ_4 decrease slowly and monotonically over the reaction path. Clearly the total energy decrease is related to the lowering of these energy levels, ψ_1 to ψ_5, especially ψ_1 the highest bonding orbital.

The variations in the major atomic orbital constituents of molecular orbitals ψ_1, ψ_3 and ψ_5 over the reaction steps are plotted in Fig. 10. Molecular orbitals ψ_2 and ψ_4 always maintain the same dominant contributions, i.e., the d_{yz} and d_{xy} orbitals

of palladium, respectively. The atomic orbital contributions of ψ_1, ψ_3 and ψ_5, on the other hand, change quite significantly. Initially, all these three molecular orbitals possess varying contributions from the palladium d_{xz} and d_{z^2} orbitals. ψ_3 becomes nonbonding with regard to ethylene–hydrogen interactions as the reaction proceeds. During steps 2–5 the Pd d_{z^2} contribution is dominant; however, at the final step the orbital is largely Pd d_{xz} in character. The hydrogen s orbital character of this molecular orbital is not given in Fig. 10 because it merely decreases over the reaction coordinate. There is a significant contribution from the C_2 p_z orbital whose participation reaches a maximum at step 2. With the movement of the ethylene there is interaction with the Pd d_{xz} orbital before bonding with the hydrogen commences. Hence the role of the Pd d_{xz} orbital is to provide a "bonding platform" for the C_2 p_z orbital while the ethylene moves from one coordination site to another. Thus, energy is not needed to break the Pd–C_2 bond before the ethylene can be transferred.

Molecular orbitals ψ_1 and ψ_5 show many similarities; both display an increase in the participation of hydrogen s orbital and Pd d_{xz} orbital over the middle stages of the reaction. Also the p_x and p_z orbitals of C_1 play an increasingly important role in both molecular orbitals as the reaction proceeds. This is especially true of ψ_1 where initially the C_1 p_z orbital is prominent, as the movement of ethylene occurs. The C_1 p_x orbital portion increases until at step 3 the contributions are equal. As the reaction continues the p_x coefficient further increases while the p_z contribution decreases. It would appear, therefore, that the Pd d_{xz} orbital is acting as a transfer orbital and this is so. The behavior of the H_s–Pd d_{xz}, C_1 p–Pd d_{xz} and C_2 p–Pd d_{xz} bond indices over the seven reaction steps are recorded in Table 6. It can be seen that in the initial stages of the reaction all three interactions are important. The H s–Pd d_{xz} and C_2 p–Pd d_{xz} bond indices show a decline after step 1 when the C_2–H interaction becomes substantial. The C_1 p–Pd d_{xz} bond index reaches a maximum at step 4 after which the C_1 p orbitals bond with the Pd p and d orbitals lying in the xp plane. The role of the Pd d_{xz} orbital is to provide a bonding interaction for the H s and the C_1 P_z orbitals before they bond with C_2 and Pd, respectively. The conduct of the Pd $d_{x^2-y^2}$ orbital in ψ_1 over the reaction path is worthy of note. During the initial stages of the ethylene movement, it is bonding with respect to the hydrogen. At step 3, however, it is antibonding with regard to the hydrogen but bonding with respect to the C_1 P_x orbital. At the end of the movement this latter interaction provides the major contribution of ψ_1.

From Fig. 9 it is seen that ψ_1 and ψ_5 pass through an energy maximum and energy minimum precisely at the position intermediate between the z and x axis (the trigonal bipyramidal structure). At this point the antibonding contributions of Pd–C_1 present in ψ_1 almost cancel the bond-

TABLE 7

Variation of Atomic Charges over the Reaction Steps of the Collapse Reaction

Atom	Reaction step						
	0	1	2	3	4	5	6
Pd	+0.152	+0.144	+0.179	+0.278	+0.173	+0.125	+0.101
H	−0.222	−0.253	−0.290	−0.386	−0.207	−0.077	+0.024
C_1	−0.049	−0.076	−0.092	−0.210	−0.199	−0.185	−0.172
C_2	−0.067	−0.073	−0.048	+0.310	+0.420	−0.013	−0.090

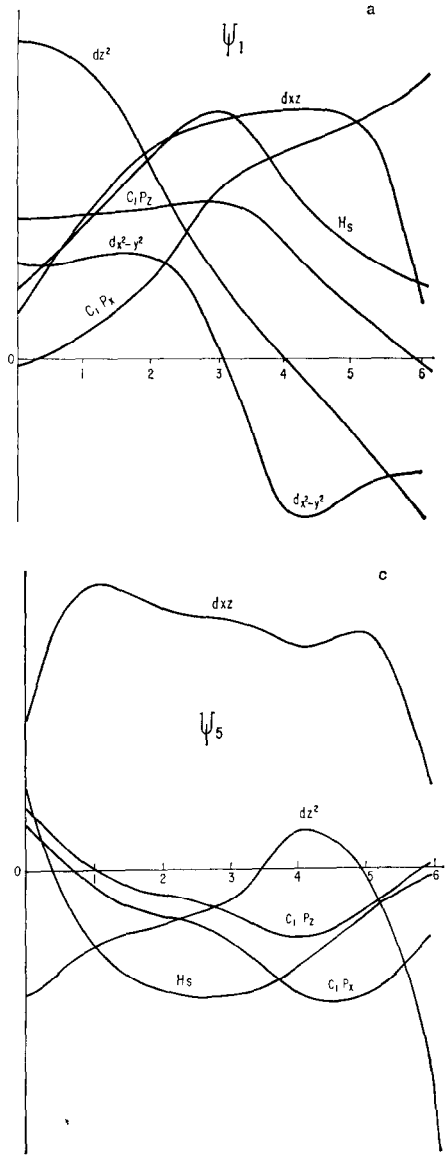

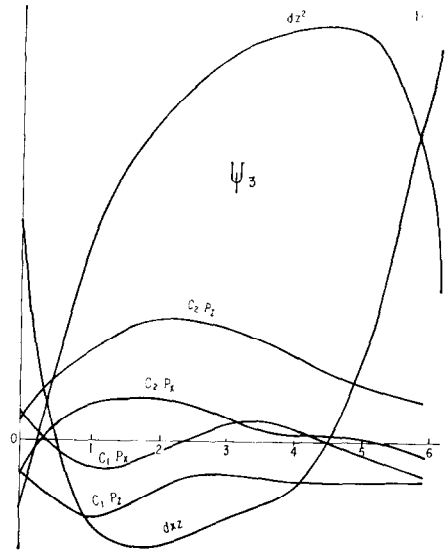

FIG. 10. Dominant atomic orbital contributions to the following molecular orbitals: (a) ψ_1; (b) ψ_3; (c) ψ_5.

ing contributions of Pd–C_1 found in ψ_5 and hence provide an explanation for the low bond index of Pd–C_1 observed in Fig. 7.

d. Liberation of the Product and Catalyst Regeneration

The last stage of the overall reaction consists simply of the attack of HCl on the final complex of Fig. 6, i.e., on the Pd–alkyl bond. The hydrogen reacts with the alkyl moiety to form the alkane while the chlorine enters the coordination sphere of palladium and regenerates the original $[PdCl_4]^{2-}$ complex. As the mechanism implies no specific catalyst action we did not calculate the reaction coordinate in detail. Figures 11 and 12 portray the electronic structures of $[\text{alkyl-}PdCl_3]^{2-}$ and $[\text{alkyl-}PdCl_3]^{2-}\cdot HCl$, respectively. In the latter species the HCl was coordinated at a distance of 2 Å from the palladium and positioned along the x-axis so that the z-axis coincided with the midpoint of the H–Cl bond.

In the case of $[\text{alkyl } PdCl_3]^{2-}$ we can see that the α-carbon atom possesses excess charge while the palladium is positively charged. Furthermore, the calculated valencies of Pd and C_1 are 2.62 and 3.69, respectively, indicating relative unsaturation at these atoms and readily implying that these atoms are points of attack for the HCl. On addition of HCl, a weakening occurs in the Pd–C_1 and H–Cl bonds while the appearance of the new Pd–Cl and H–C_1 bonds is significant. Hence we envisage this reaction stage to proceed with increased weakening and strengthening of

these afore-mentioned bonds, respectively, by the parallel lengthening and shortening of the appropriate bond distances. Indeed we find that as the complex of Fig. 11 rearranges to a four-center transition state, a more stable state is obtained.

The charges on the atoms at the seven steps of the previous stage are presented in Table 7. A survey of these values reveals that the negative charge on the α-carbon atom reaches a maximum at the middle step and remains high to the end. This implies that the above attack by HCl could happen before the olefin has completed its collapse to the x-axis. This possibility is based both on the attainment of a maximum negative charge on the α-carbon atom and of a minimum in the Pd–alkene bond order at the intermediate position of the reaction coordinate of Fig. 6. (i.e., the trigonal bipyramidal situation).

CONCLUSIONS

The main features of the mechanism discussed above are the demonstration of the capability of the $[PdCl_4]^{2-}$ complex to produce a heterolytic breaking of H_2, the description of the movement of the coordinated olefin towards the hydrogen (collapse mechanism), and the explanation, through the charge distribution, of the attack of HCl on the coordinated alkyl.

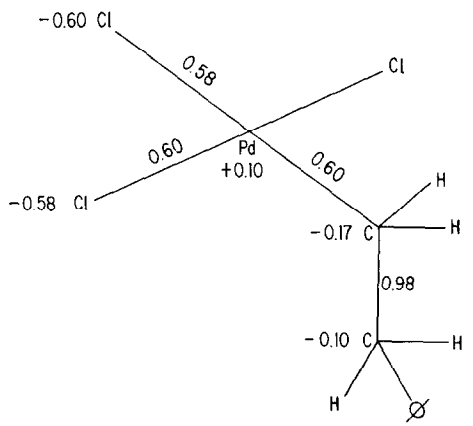

FIG. 11. Charge distribution of $[alkyl\text{-}PdCl_3]^{2-}$.

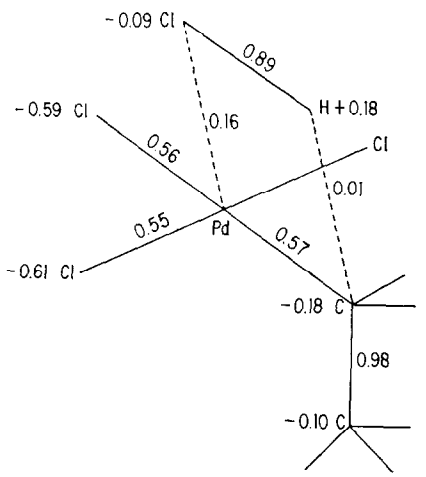

FIG. 12. Charge distribution of $[alkyl\text{-}PdCl_3]^{2-} \cdot HCl$.

The collapse process merits a more detailed discussion. It has been shown that in catalytic reactions involving *cis*-migration of one of the reactants, the molecular orbital analysis always indicates that the bond between this reactant and the metal is quite labile (*7*, *8*). Furthermore we find that such a bond is generally associated with the highest occupied molecular orbital. In the present calculations a different situation arises. The molecular orbital that gives a bonding contribution to the Pd–styrene bond is rather low (orbital ψ_5 in Fig. 9). The highest occupied orbital is in fact antibonding between palladium and styrene. This apparent difference with previously studied catalyzed reactions permits, however, the establishment of a common description of all these processes. In all cases we have a labile bond which in the present calculations comes from the contributions of a bonding and an antibonding molecular orbital. We here propose that this is a consequence of the very transient nature of the over-coordinated complexes. The involved metals only support the higher coordinated structure (pentacoordination for palladium or platinum and hexacoordination for titanium) as an unstable situation which soon collapses to a lower coordination (square planar structures for palla-

dium or platinum, and trigonal bipyramidal for titanium). It is our conclusion that the high activity that such catalysts present is a measure of their tendency to reduce their coordination number. The role played by *d* orbitals as transfer agents for ligands in order to attain this lower coordination number is therefore very critical.

One interesting characteristic of the $[PdCl_4]^{2-}$ catalyst is the significance attached to the two anionic electrons. We have seen, in fact, that the two extra electrons occupy the antibonding orbital, i.e., they effectively labilize the palladium–olefin bond. This situation is not altered by solvent or support effects, as these tend to balance the overall charge but *do not alter* the charge population of the complex itself.

ACKNOWLEDGMENTS

We sincerely thank the IMP Computing Department and especially Ings. A. Garcia del Busto and J. D. Gonzalez for their collaboration. One of us (D. R. A.) expresses his gratitude to the National University of Mexico and the Institute Mexicano del Petroleo for their hospitality.

1. Herberhold, M., "Metal π-Complexes." Elsevier, London, 1974.
2. Linarte, R., Perez-Villagomez, H., and Ruizvizcaya, M. E., unpublished data.
3. Germain, G. E., and Linarte, R., *Bull. Soc. Chem.* (*Fr.*) **5**, 1869 (1971).
4. Linarte, R., *Acta Cient, Venz. Suppl.* **24**, 239 (1973).
5. Linarte, R., Valle, J., and Cuatecontzi, D. H., "Catalysis: Heterogeneous and Homogeneous," pp. 467–488. Elsevier, London, 1975.
6. Armstrong, D. R., Perkins, P. G., and Stewart, J. J. P., *J. Chem. Soc. A* 3654 (1971).
7. Armstrong, D. R., Perkins, P. G., and Stewart, J. J. P., *J. Chem. Soc. A* 1972 (1972).
8. Novaro, O., Chow, S., and Magnouat, P., *J. Catal.* **42**, 131 (1976), and references therein.
9. Armstrong, D. R., Fortune, R., and Perkins, P. G., *J. Catal.* **42**, 435 (1976).
10. Armstrong, D. R., Fortune, R., and Perkins, P. G., unpublished data.
11. "Interatomic Distances in molecules and Ions," *Chem. Soc. Special Publ.* No. 11, London, 1958.
12. Fryer, C. W., and Smith, J. A. S., *J. Chem. Soc. A* 1029 (1970).
13. Harris, C. M., Livingstone, S. E., and Reece, I. H., *J. Chem. Soc.* 1505 (1959).
14. Gray, H. B., and Ballhausen, C. J., *J. Amer. Chem. Soc.* **85**, 260 (1963).
15. Day, P., Orchard, A. F., Thompson, A. J., and Williams, R. J., *J. Chem. Phys.* **42**, 1973 (1965).
16. Armstrong, D. R., Perkins, P. G., and Stewart, J. J. P., *J. C. S. Dalton* 838 (1973).
17. Armstrong, D. R., Perkins, P. G., and Stewart, J. J. P., *J. C. S. Dalton* 2273 (1973).
18. Taqui Khan, M. M., and Martell, A. E., "Homogeneous Catalysis by Metal Complexes," Academic Press, New York, 1974.
19. Cossee, P., *J. Catal.* **3**, 80 (1964).
20. Novaro, O., Chow, S., and Magnouat, P., *J Polym. Sci.*, **13**, 761 (1975).